

Rational Design of Chiral Nanoscale Adamantanoids

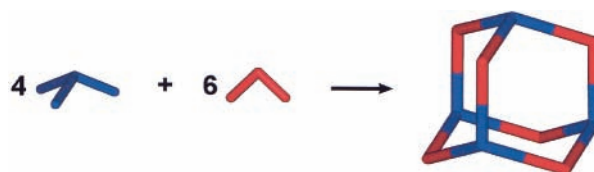
Manuela Schweiger, S. Russell Seidel, Marion Schmitz, and Peter J. Stang*

Department of Chemistry, University of Utah, 315 S. 1400 E.,
Salt Lake City, Utah 84112

stang@chemistry.utah.edu

Received March 9, 2000

ABSTRACT



Utilizing coordination as a motif, the self-organization of six ditopic and four tritopic building blocks leads to the formation of nanoscale adamantanoid frameworks.

Self-assembly via rational design has led to a fascinating variety of two- and three-dimensional supramolecular structures. Such species are formed and held together by the noncovalent or dative interactions of predesigned building blocks. One approach exploits transition-metal-mediated self-organizing processes, in which the coordination of suitable precursors serves as a viable recognition motif.¹ This methodology allows for the preparation of complex, nanoscopic² supramolecules of predetermined shape, size, and functionality.³

(1) (a) Leininger, S.; Olenyuk, B.; Stang, P. J. *Chem. Rev.* **2000**, *100*, 853. (b) Caulder, D. L.; Raymond, K. N. *J. Chem. Soc., Dalton Trans.* **1999**, 8, 1185. (c) Caulder, D. L.; Raymond, K. N. *Acc. Chem. Res.* **1999**, *32*(11), 975. (d) Chambron, J.-C.; Dietrich-Buchecker, C.; Sauvage, J.-P. Transition Metals as Assembling and Templating Species. In *Comprehensive Supramolecular Chemistry*; Lehn, J.-M., Chair Ed.; Atwood, J. L., Davis, J. E. D., MacNicol, D. D., Vögtle, F., Exec. Eds.; Pergamon Press: Oxford, 1996; Vol. 9, Chapter 2, p 43. (e) Baxter, P. N. W. Metal Ion Directed Assembly of Complex Molecular Architectures and Nanostructures. In *Comprehensive Supramolecular Chemistry*; Lehn, J.-M., Chair Ed.; Atwood, J. L., Davis, J. E. D., MacNicol, D. D., Vögtle, F., Exec. Eds.; Pergamon Press: Oxford, 1996; Vol. 9, Chapter 5, p 165. (f) Fujita, M.; Ogura, K. *Coord. Chem. Rev.* **1996**, *148*, 249. (g) Fujita, M. *Chem. Soc. Rev.* **1998**, *6*, 417. (h) Saalfrank, R. W.; Bernt, I.; Uller, E.; Hampel, F. *Angew. Chem., Int. Ed.* **1997**, *36*, 2482. (i) Baxter, P. N. W.; Lehn, J.-M.; Baum, G.; Fenske, D. *Chem. Eur. J.* **1999**, *5*, 102. (j) Stang, P. J.; Olenyuk, B. *Acc. Chem. Res.* **1997**, *30*, 502.

(2) Philp, D.; Stoddard, J. F. *Angew. Chem., Int. Ed. Engl.* **1996**, *35*, 1154.

(3) (a) Kusakawa, T.; Fujita, M. *J. Am. Chem. Soc.* **1999**, *121*, 1397. (b) Ibukuro, F.; Kusakawa, T.; Fujita, M. *J. Am. Chem. Soc.* **1998**, *120*, 8561.

The hydrocarbon adamantane⁴ has been well-known since its discovery in petroleum residues in the 1930s. Its framework is composed of four six-membered rings that are fused nearly strain-free in their thermodynamically most favored chair conformations. With its crystal lattice consisting of an infinite adamantanoid network, the high-pressure carbon allotrope diamond⁵ is also structurally related to this compound.

To date, the only examples of *self-assembled* adamantanoids have been reported by Saalfrank, et al.⁶ These systems exploit chelating effects between bidentate angular subunits and various alkaline earth and transition metals. In our approach, supramolecular adamantanoids are designed according to the “Molecular Library” model.^{1a} By combining six angular ditopic units (A²), such as **1**, with four angular tritopic units (A³), such as **2**, an A²₆A³₄ entity arises. Provided that the angles are all approximately 109°, an adamantanoid

(4) Fort, R. C.; Schleyer, P. R. *Chem. Reviews* **1964**, *64*, 277.

(5) Angus, J. C.; Hayman, C. C. *Science* **1988**, *4868*, 913.

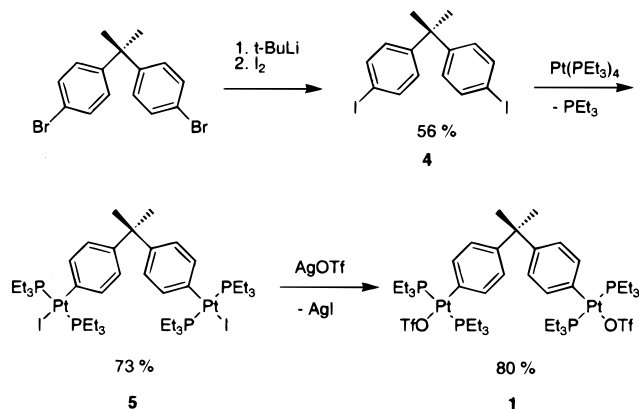
(6) (a) Saalfrank, R. W.; Stark, A.; Peters, K.; von Schnering, H. G. *Angew. Chem., Int. Ed. Engl.* **1988**, *27*, 851. (b) Saalfrank, R. W.; Stark, A.; Bremer, M.; Hummel, H.-U. *Angew. Chem., Int. Ed. Engl.* **1990**, *29*, 311. (c) Saalfrank, R. W.; Burak, R.; Breit, A.; Herbst-Irmer, R.; Daub, J.; Porsch, M.; Bill, E.; Müther, M.; Trautwein, A. X. *Angew. Chem., Int. Ed. Engl.* **1994**, *33*, 1621. (d) Saalfrank, R. W.; Burak, R.; Reihls, S.; Löw, N.; Hampel, F.; Stachel, H.-D.; Lentmaier, J.; Peters, K.; Peters, E.-M.; von Schnering, H. G. *Angew. Chem., Int. Ed. Engl.* **1995**, *34*, 993. (e) Saalfrank, R. W.; Löw, N.; Demleitner, B.; Stalke, D.; Teichert, M. *Chem. Eur. J.* **1998**, *4*, 1305.

framework results. As building block **2** has a stereogenic center in its carbon backbone, its assembly with tecton **1** leads to the first optically active adamantanoid.⁷ Moreover, this aggregate serves as the first example of an adamantanoid to have a nanoscale internal cavity.

To test the limits of the structural design and the allowable flexibility of the ditopic building block, the reaction of tecton **3** with tritopic linker **2** was probed. Although **3**, with its 120° angle, does not fulfill the ideal requirements, the deviation is apparently not substantial enough to prevent the self-organization of the subunits into an adamantanoid, as spectroscopic data reveal.

Platinum containing linker **1** is prepared as shown in Scheme 1. A halogen exchange is carried out by reacting

Scheme 1. Synthesis of Ditopic 109° Corner Unit



2,2-bis(4-bromophenyl)propane⁸ with *tert*-butyllithium and I₂ to yield compound **4**. Via 2-fold oxidative addition, Pt(PEt₃)₄ is inserted (**5**), followed by subsequent reaction with AgOTf. As a result, bistriflate **1** can be isolated in good yield. Precursor **3** has been prepared according to previously published literature.⁹

To synthesize an adamantanoid, a complementary tritopic subunit A³ is required. Compound **2**, which fills this role, is synthesized by reacting lithiated tris(4-pyridyl)methanol¹⁰ with 2-(*R*)-phenylbutyryl chloride.¹¹ The corresponding chiral ester **2** emerges in 25% yield as depicted in Scheme 2.

By combining dilute CD₂Cl₂ solutions of **1** or **3** with **2** in the proper 6:4 ratio, adamantanoids **6** and **7** form, respectively, in quantitative yield as determined by NMR (Scheme 3). The self-organization of these species is instantaneous

(7) (a) Stang, P. J.; Olenyuk, B.; Muddiman, D. C.; Smith, R. D. *Organometallics* **1997**, *16*, 3094. (b) Fuss, M.; Siehl, H.-U.; Olenyuk, B.; Stang, P. J. *Organometallics* **1999**, *18*, 758. (c) Müller, C.; Whiteford, J. A.; Stang, P. J. *J. Am. Chem. Soc.* **1998**, *120*, 9827. (d) Fan, J.; Whiteford, J. A.; Olenyuk, B.; Levin, M. D.; Stang, P. J.; Fleischer, E. B. *J. Am. Chem. Soc.* **1999**, *121*, 2741.

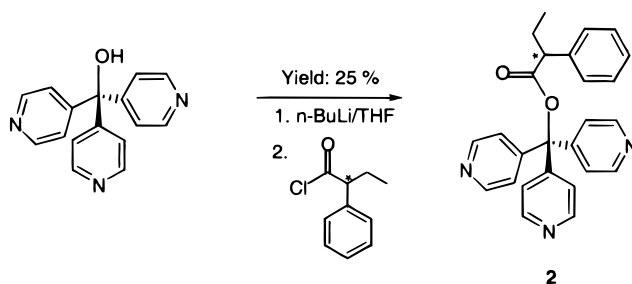
(8) Van Walree, C. A.; Roest, M. R.; Schuddeboom, W.; Jennekens, L. W.; Verhoeven, J. W.; Warman, J. M.; Kooijman, H.; Spek, A. L. *J. Am. Chem. Soc.* **1996**, *118*, 8395.

(9) Leininger, S.; Schmitz, M.; Stang, P. J. *Org. Lett.* **1999**, *1*, 1921.

(10) Olenyuk, B.; Levin, M. D.; Whiteford, J. A.; Shield, J. E.; Stang, P. J. *J. Am. Chem. Soc.* **1999**, *121*, 10434.

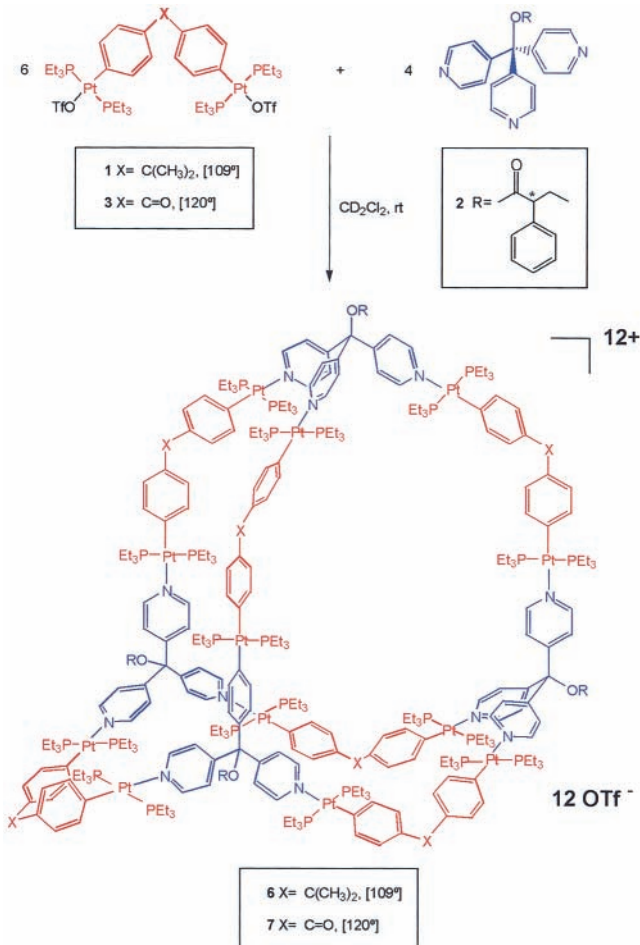
(11) Jones, P. R.; Goller, E. J.; Kauffman, W. J. *J. Org. Chem.* **1971**, *36*, 3311.

Scheme 2. Preparation of Chiral, Tritopic 109° Tecton



and can be monitored by multinuclear NMR. Of particular diagnostic value are the ¹H and ³¹P{¹H} NMR spectra of **6** and **7**, which indicate the formation of highly symmetrical structures. Furthermore, in both cases the relative shifts of these resonances are comparable in both direction and absolute value. The protons in the positions α and β to the pyridine-N both exhibit downfield shifts due to the loss of electron density upon coordination. The shifts for the α-pyridyl protons were 0.19 ppm for **6** and 0.26 ppm for **7**, while the resonances of the β-pyridyl protons experience a stronger influence with shifts of 0.66 ppm in the case of **6**

Scheme 3. Self-Assembly of the Adamantanoids



and 0.74 ppm in that of **7**. As a result of increased back-donation from the platinum to the phosphine moiety, the protons of the methylene groups bonded to the phosphorus show almost identical upfield shifts, 0.34 and 0.33 ppm, for both compounds **6** and **7**, respectively. The $^{31}\text{P}\{^1\text{H}\}$ signals themselves are shifted upfield by 5.6 ppm ($J_{\text{Pt-H}} = 2652$ Hz) for **6** and 5.3 ppm ($J_{\text{Pt-H}} = 2670$ Hz) for **7** relative to starting materials **1** and **3**. $^{13}\text{C}\{^1\text{H}\}$ and ^{19}F NMR spectra are both consistent with the proposed structure.

Electrospray ionization mass spectrometry has proven to be an indispensable tool in the corroboration of structural assignments for self-assembled aggregates of this nature.¹² Both species **6** and **7** show similar peak and fragmentation patterns, lending further evidence to their structural similarity. Peaks attributable to the consecutive loss of triflate counterions, $[\text{M} - 3\text{OTf}]^{3+}$ $\{m/z = 3107$ for **6** (calcd 3105) and 3079 for **7** (calcd 3077)}, $[\text{M} - 4\text{OTf}]^{4+}$ $\{m/z = 2293$ for **6** (calcd 2292) and 2272 for **7** (calcd 2271)}, and $[\text{M} - 5\text{OTf}]^{5+}$ $\{m/z = 1805$ for **6** (calcd 1804) and 1788 for **7** (calcd 1787)}, where M represents the intact adamantanoid cage, were detected. Furthermore, several fragments could be identified, with the most dominant among them consisting of a +1 charged 1:1 composition of **2** and **1** or **3** minus one OTf $\{m/z = 1616$ for **6** (calcd 1615) and 1601 for **7** (calcd 1601)}. When combined with the information obtained from NMR measurements, this mass spectral data provides strong support for the proposed structures of **6** and **7**.

Both **6** and **7** should be optically active, given that they each contain four of the chiral building blocks **2**. Optical rotation studies indicate that this is indeed the case. Moreover, the molarity-based specific rotation, $[\phi]_{\text{D}}$, is enhanced compared to that of starting unit **2** (−122) with values of −261 for **6** and −1168 for **7**.

As suitable X-ray quality crystals could not be obtained, MM2 force field simulations¹³ were employed to visualize both the size and shape of these three-dimensional cages. The calculated structure of adamantanoid **6** is displayed in Figure 1. As a result of the stereogenic centers present in the backbone of the ester moiety, the symmetry of **6** and **7** is reduced, with D_2 symmetry as opposed to the T_d symmetry

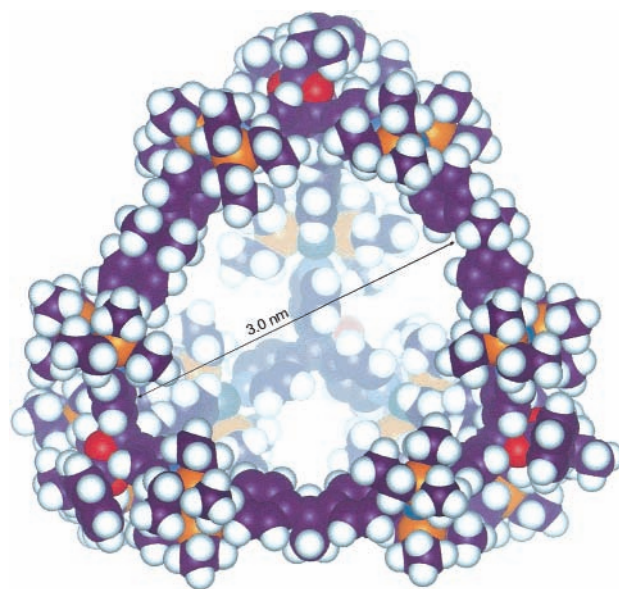


Figure 1. MM2 force field simulation of adamantanoid **6**.

expected for achiral adamantanoids. The diameter of the inner cavity of the cage along one of the C_2 -axes is approximately 3 nm.

In conclusion, herein we report the first self-assembled adamantanoid cages that are chiral and in the nanoscale range. These molecular architectures represent further unique members in the growing family of large supramolecular entities, illustrating the versatility of an angle-directed, transition-metal-mediated approach.

Acknowledgment. We thank the National Institute of Health (5R01GM57052) for support, the Austrian Foundation for Scientific Research (FWF) for an Erwin Schrödinger Fellowship for Manuela Schweiger, and the Alexander von Humboldt Foundation for a Feodor Lynen Fellowship for Marion Schmitz.

Supporting Information Available: General experimental procedures and characterization data for compounds **6** and **7**. This material is available free of charge via the Internet at <http://pubs.acs.org>.

OL005781N

(12) (a) Whiteford, J. A.; Lu, C. V.; Stang, P. J. *J. Am. Chem. Soc.* **1997**, *119*, 2524. (b) Stang, P. J.; Cao, D. H.; Chen, K.; Gray, G. M.; Muddiman, D. C.; Smith, R. D. *J. Am. Chem. Soc.* **1997**, *119*, 5163. (c) Constable, E. C.; Schofield, E. *J. Chem. Soc., Chem. Commun.* **1998**, 403.

(13) *Chem3D Pro 3.5.2*; CambridgeSoft Corporation: U.S., 1996.